GeoChronicle Panorama, Vol.3, No.1, December 2023 pp.24-36

Banded Iron Formations and Their Economic Prospects with Special Reference to India

Saptarshi Banerjee*
PG-II, Department of Geology, Presidency University
86/1 College Street, Kolkata-700073, W.B., India
*Corresponding email: saptarshi11012000@gmail.com

Abstract: Banded iron formations (or the acronym BIFs) are marine chemical sediments consisting of centimeter-thick interlayered alternating bands of chert and iron-rich minerals with granules and oolites or laminations (including micro-banding) as texture, were deposited throughout much of the Precambrian era via a unique confluence of atmospheric, hydrospheric, lithospheric, and biospheric conditions where microorganisms may have played an important role in their genesis. Banded Iron Formation (BIF) and associated iron ore deposits occupy three distinct provinces (best-preserved basins of the Precambrian period that form Iron Ore Super Group) surrounding the North Odisha Iron Ore Craton (NOIOC) located in eastern India and have been studied in detail along with the geochemical evaluation of different iron ores, suggests that the massive, hard laminated, soft laminated iron ore intricately related with the Banded hematite jasper had a genetic lineage from BIFs aided with certain input from hydrothermal activity. In the present scenario, the Indian Steel industry is totally dependent upon high-grade iron ore. Due to the high demand for good quality iron ores and the rapid depletion of high-grade ores, it has necessitated to emphasize on beneficiation of lean ores like banded hematite jasper (BHJ) and banded hematite quartzite (BHQ) as alternate resources of iron ore.
Key Words: Banded Iron Formations, Composition, Distribution, Genesis, North Odisha Iron ore Craton, India.

Prologue

Banded iron formations form one of the earth's mineral treasures. Besides the term BIF, these rocks are known in different continents under the terms itabirite, jaspilite, hematite-quartzite, and specularite (Evans, 1993). No model to explain the origin of banded iron formations has won unanimous acceptance The banded appearance is caused by the intimate interbedding of mm to cm thick beds of dark gray to black iron oxides and red to maroon chert/jasper (Fig. 1). They occur in stratigraphical units hundreds of metres thick and hundreds or even thousands of kilometers in lateral extent. Substantial parts of these iron formations are usable directly as low-grade iron ore (e.g., taconite) and other parts have been the protores for higher grade deposits. Compared with the present enormous demand for iron ore, now approaching 109 t p.a., the reserves of mineable ore in the banded iron formations are very large indeed (James and Sims, 1973). An extraordinary fact emerging from recent studies is that the enormous bulk of iron formations of the world has an amount of at least 1014 t and possibly 1015 t, i.e., 90% or more of the total BIF in the Precambrian, was laid down in the very short time interval of 2500-1900 Ma ago (James and Trendall, 1982) and now represented by the BIF of Labrador, the Lake Superior region of North America, Krivoi Rog and Kursk, USSR and the Hamersley Group of Western Australia. Although BIF is important in the Archaean, it could not be developed on the large scale seen in the early Proterozoic because stable continental plates were not generally present. Following the development of stable lithospheric plates, BIF could be laid down synchronously over very large areas; this took place possibly in intra-plate basins and certainly on continental shelves. The Archaean BIFs are generally the Algoma type, that is present and this BlF development reached a peak in the late Archaean, and occurs both in high-grade gneiss terranes and greenstone belts. In contrast to all other Precambrian areas, China has uniquely large and significant gneiss-hosted Archaean BIF deposits. This current paper represents a brief review of potential pathways, in the genesis of great Precambrian BIF deposition by critically examining the substantial articles published, so far, related to this topic and their economic significances with special reference to Indian occurrences, reserve potential of different types of iron ore and uses.

Mineralogy

The composition of BIF is dominated by silica (~40–50%) and iron (~20–40%). They are considered to be of sedimentary origin but always display a diagenetic and metamorphic overprint which sometimes significantly altered the original sediment in terms of its composition and mineralogy. Therefore, the main minerals phases now found in BIF, such as hematite (Fe_2IIIO_3), magnetite ($Fe_2IIIFeIIO_4$), chert (SiO_2) and stilpnomelane ($K(FeIIMg, FeIII)_8(Si,Al)_{12}(O,OH)_{27}$) are actually of secondary origin. Proposed primary minerals are ferric hydroxide ($Fe(OH)_3$), siderite ($FeII(CO_3)$) (partially secondary), greenalite ($(Fe)_3Si_2O_5(OH)_4$) and amorphous silica (Klein 2005).The iron in BIF originated as dissolved Fe(II) from submarine hydrothermal vents and was subsequently transformed to dissolved Fe(III) in the upper water column by either abiological or biological oxidation. The ferric iron then hydrolysed rapidly to ferric hydroxide and settled to the sea floor where further transformations ensued.

An early BIF categorization was done by James, who classified BIF about their mineralogy. Carbonate-dominated BIF usually contains alternating chert and inorganic carbon-rich mineral layers, the latter composed of ankerite ($Ca(Fe, Mg, Mn)(CO_3)_2$) and siderite. Those with a high amount of hematite and magnetite are classified as oxide-rich BIF, but they may also contain subsidiary amounts of siderite and iron silicates. Silica-rich BIF are dominated by chert, a variety of silicate minerals, such as stilpnomelane, minnesotaite ($(Fe, Mg)_3Si_4O_{10}(OH)_2$), greenalite, and carbonates.

(a) (b) (c)

Fig. 1. (a) 2.1 billion-year-old BIF from North America in the Dresden Botanical Garden, Germany, (b) BIF consists of repeated, thin layers (a few mm to a few cm in thickness) of silver to black iron oxides, either magnetite (Fe_3O_4) or hematite (Fe_2O_3), alternating with bands of iron-poor shales and cherts, often red in colour, of similar thickness, and containing microbands (sub-mm) of iron oxides, (c) Folded and metamorphosed Superior type banded iron formation near Mt Tom Price mine in the Hamersley Gorge, Western Australia with iron-rich beds in black, silica (jasper) in red (Source: Pohl, 2011; Neukirchen and Gunnar, 2020).

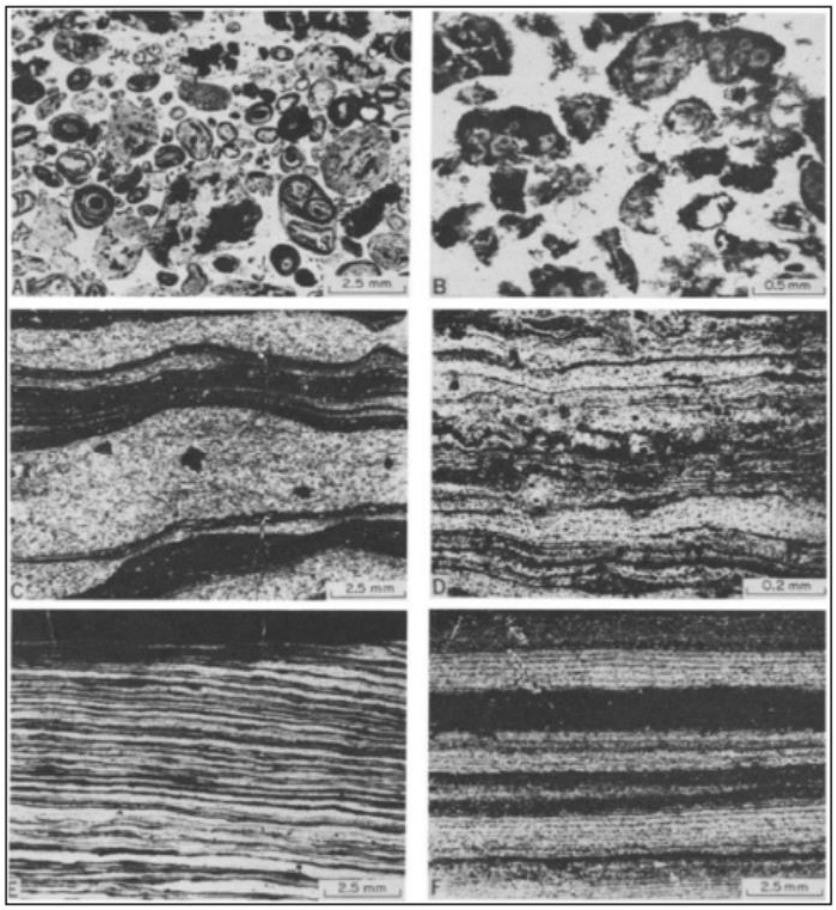

Fig. 2. Dominant small-scale structures in Precambrian banded iron formations. (a) Oolites and granules composed of magnetite, chert, minor carbonate, and stilpnomelane in a chert-rich matrix. (b) Granules of minnesotaite, greenalite, stilpnomelane, siderite, and minor magnetite in a chert-rich matrix. (c) Laminae in a minnesotaite-stilpnomelane-quartz minor magnetite assemblage. (d) Microbands are defined by quartz, magnetite and minor siderite, ankerite and chlorite. (e) Microbanding in a quartz-magnetite mesoband. (f) Alternating massive and microbanded mesobands in a magnetite-quartz-minor grunerite bearing iron-formation, metamorphosed to amphibolite grade (Source: Gole and Klein, 1981).

Sedimentary Structures and Texture

As the name implies, most banded iron formations have well-developed thin lamination (mm or fractions of a mm) to thin bedding (0.5-3 cm) with alternating iron-rich and iron-poor layers (Fig. 1). Thin lamination is the norm in fine-grained Precambrian strata, given the lack of burrowers, but the layers in banded iron formations (particularly those rich in iron oxides) are among the most striking found in sediments of any age. Bedding can also be highly cyclic via the alternation of either iron-rich vs. iron-poor layers within BIF or layers of BIF vs. layers of fine shaly or volcaniclastic sediment (Trendall and Blockley, 1970). The only common sedimentary structures in banded iron formations other than banding are chert pods, which are concretion-like bodies rich in silica that are typically ellipsoidal in cross-section. Individual layers can often be traced continuously through chert pods. Drastic changes in the thickness of individual layers that pass through chert pods indicate that some, and perhaps most, silica-poor banded iron formations lost 90% or more of their original thickness during compaction. Precambrian BIFs may contain oolites, granules, and other fragments embedded in a matrix, and they may be finely banded as well (Fig. 2a and 2b). Iron formations containing oolites and granules appear to be almost solely restricted to the Proterozoic as these structures have rarely been observed in Archean BIFs. In this paper, we have adopted the definitions of Trendall and Blockley (1970) for various scales of banding: macrobands are coarse alternations of contrasting rock types; mesobands tend to have an average thickness of less than an inch; and microbands usually range from 0.3 to 1.7mm. Trendall (1965) has defined microbanding as the alternation of one Fe-rich with one chert-rich lamina constituting a single microband. The laminated and granular parts of iron formations generally occur in different macro bands. From descriptions in the literature and our own limited observations, it appears that lamination is most commonly expressed by alternating 0.1-2.0mm thick laminae of different Feminerals (Fig. 2c) and that microbanding in the strict sense is very uncommon. Generally, only quartz or chert-rich mesobands are microbanded (Fig. 2d, 2e and 2f) because the laminated members consist mainly of Fe-silicate and carbonate-rich assemblages.

Banded iron formations originally consisted of a broad spectrum of iron-rich minerals in precipitates that were too fine-grained to reveal much via petrographic analysis. The fine-grained texture indicates that the particles, precipitated originally must have been quite small. Most of these minerals are thought to have compositions close to the phases originally precipitated from basin waters, except for stilpnomelane and other aluminosilicate minerals. Aluminous minerals in either banded or granular iron formations usually reflect contamination with volcaniclastic and/or siliciclastic detritus. Exquisite volcanic shards replaced by stilpnomelane occur in some iron formations. Finally, the abundance of silica at a given stratigraphic level can vary tremendously along bedding; this generally takes the form of what are known as chert pods.

Tectonic Setting

BIF is broadly classified according to tectonic setting, size, and lithology as either Algoma or Lake Superior type (Gross, 1965) (Fig. 3). Algoma-type BIFs (mostly 3.5–3 billion years old) are often replaced by volcanic rock sequences and occur mainly in Archean greenstone belts together with greywacke, submarine tuffs, and volcanic rocks, suggesting a geosynclinal environment and the oxide, carbonate, and sulphide facies are present, with iron silicates often appearing in the carbonate facies. Oolitic and granular textures are absent or inconspicuous and the typical texture is a streaky lamination. They were created at different water depths (especially, at island arcs, in back arcs, and in rift systems). Their thickness and lateral expansion are usually relatively small. They are mined, for example, in the Abitibi greenstone belt in Canada. The oldest deposits of this type can be found in the Isua greenstone belt on Greenland where they have an age of about 3800 million years. Although they usually appear in the late Archean, there are also Algoma-type BIFs found in the late Proterozoic. The largest iron deposits are Superior-type BIFs (usually 2500–1900 million years old). They emerged at a time when cyanobacteria were producing ever-increasing amounts of oxygen. They formed in shelf seas, on continental slopes, or in epicontinental seas (i.e., inland seas) mostly associated with quartzites, black carbonaceous shales, and usually also with conglomerate, dolomite, massive chert, chert breccia, and argillite (Heinrich et al., 1982; Planavsky et al., 2009). Channels, desiccation cracks, cross-bedding, and ripple marks are common. Oolites and intra-clasts of iron-rich minerals are abundant. The influence of land seems small as the lack of coarse clastic sediments shows. The deposits can be very large with an extension of tens of thousands of square km and a thickness of tens or hundreds of meters. They are considered biogenic or chemical sediments because of the absence of volcanic phenomena in their vicinity but they are nearly always present somewhere in the stratigraphical column. The successions in which these BIFs occur usually lie unconformably on highly metamorphosed basement rocks with the BIF, as a rule, in the lower part of the succession, and in

some places, they are separated from the basement rocks by only a metre or so of quartzite, grit, and shale. The name is derived from the BIFs around Lake Superior (Wisconsin, Michigan, Minnesota, USA, and Ontario, Canada). The Hamersley Range (Western Australia) is the most important in the world. Another Rapitan-type BIFs (600–750 million years old) are the most recent and they always occur along with glacial sediments. They were created during large-scale glaciation (Snowball Earth scenario). This type is economically insignificant.

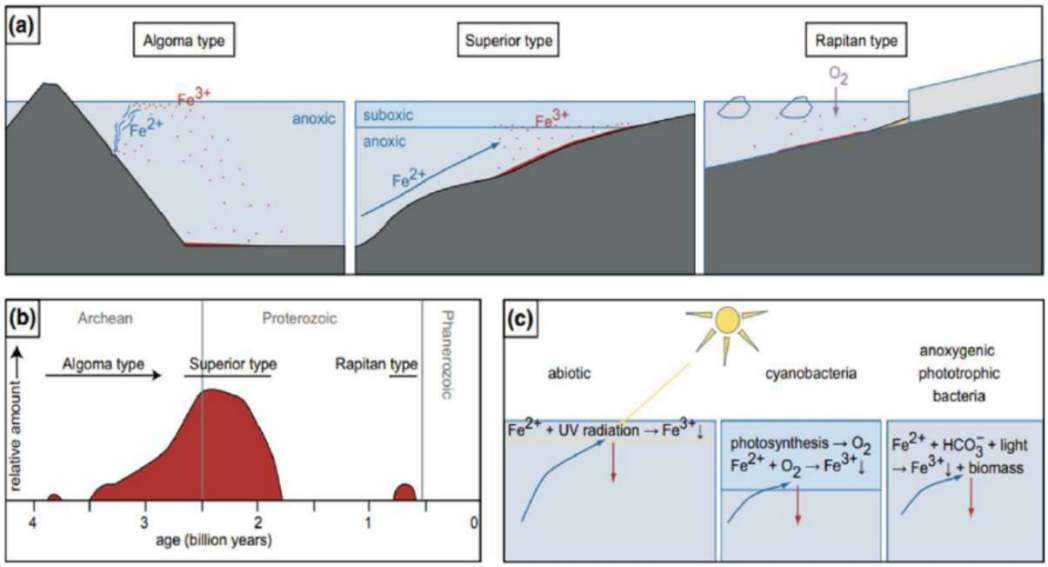

Fig. 3. (a) BIFs can be divided into three types that arose under different conditions, (b) at different times and (c) Three processes are mainly responsible for the oxidation and thus for precipitation: abiotic oxidation by UV radiation, oxidation with O_2 released by photosynthetic microorganisms, and direct oxidation by certain bacteria without O_2 (Source: Neukirchen and Gunnar, 2020).

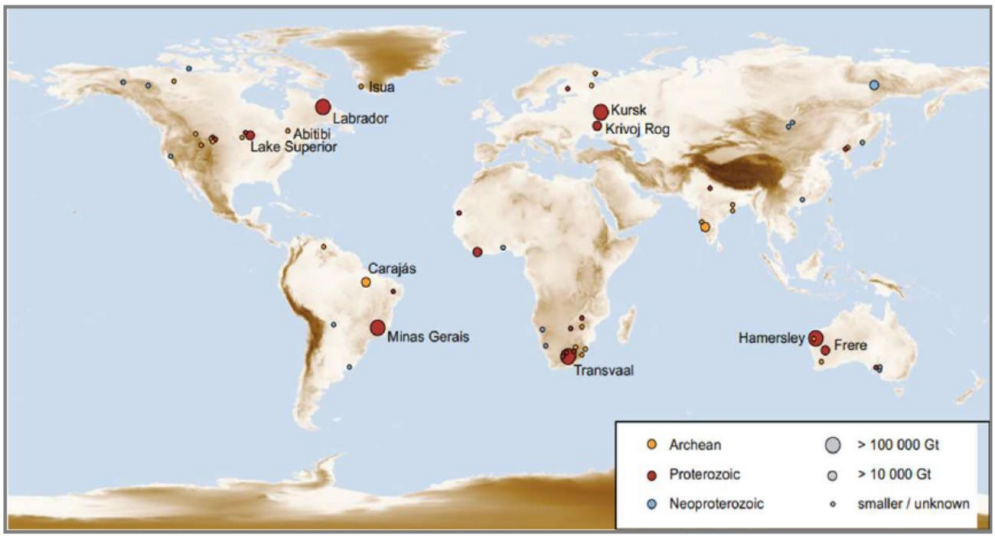

Fig. 4. Important BIFs by age and size. Their large occurrence is exclusively in the Precambrian cores of the continents. BIF, Banded iron formation (Source: Bekker et al., 2004).

Spatial and Temporal Distribution of BIF

BIFs are found worldwide, in every continental shield of every continent (Fig. 4). These are almost exclusively Precambrian in age, with most deposits dating to the late Archean (2800-2500 Ma) with a secondary peak of deposition in the Orosirian period of the Paleoproterozoic (1850 Ma). Minor amounts were deposited in the early Archean and in the Neoproterozoic (750 Ma). The oldest BIFs are those of the Isua supracrustal Belt in Western Greenland with an approximate age of ~3.8–3.9 Ga (Mojzsis et al., 1996) associated with greenstone belts. Other examples of early Archean BIFs include the Sebakwian Group in Zimbabwe with an age of ~3.2–3.6 Ga, Abitibi greenstone belts, the greenstone belts of the Yilgarn and Pilbara cratons, the Baltic shield, and the cratons of the Amazon, north China, and south and west Africa. Further Archean BIF founds in the late

Archean Vanivilas Formation in the Dharwar Supergroup in India with an age of ~2.6–2.8 Ga. The transition zone between the Archean and the Proterozoic is marked by BIF in the Transvaal Supergroup, South Africa, with an age of ~2.7–2.5 Ga. The most extensive banded iron formations belong to what A.F. Trendall calls the Great Gondwana BIFs. These are late Archean in age and are not associated with greenstone belts. They are relatively undeformed and form extensive topographic plateaus such as the Hamersley Range, where BIFs were deposited from 2470 to 2450 Ma and are the thickest and most extensive in the world, with a maximum thickness in excess of 900 meters (3,000 feet). The Gunflint and Biwabik Iron Formation in Northern America can be assigned to the Proterozoic BIF with an age of ~2.0–1.9 Ga. BIF then disappeared from the rock record until around 750 million years ago with their re-emergence in the Rapitan Group in Canada with an age of ~750 Ma. These latter BIF are associated with Snowball Earth glacial events (Hoffman and Schrag, 2000).

Origin

The sources of iron in BIFs are controversial. Previous studies suggested that the iron was derived from the weathering of terrigenous materials (James, 1954), whereas the iron in volcanogenic BIFs may be directly derived from submarine volcanic activities (Klein, 2005). Terrigenous input includes rivers, aeolian dust, glaciers, and coastal erosion. The basalt–andesite–rhyolite formed by marine volcanism is predominant in the Archean Ocean, and consequently, the volcanogenic materials have dominated the marine solute input. In addition, the higher geothermal gradient (>60 ºC/km) in the Archean promotes the strong free convection of seawater, thus forming the submarine hydrothermal system dominated by volcanic materials, which is the main source of iron (Klein, 2005). Due to the minimal involvement of organic C (carbon) in the BIF deposition, there is no evidence to support the claim that BIF deposition is directly related to microbial activities. However, many other studies have suggested that biological processes are involved in BIF deposition (Raye et al., 2015; Li et al., 2015), such as shallow-water carbonate-shale lithology in BIFs (rich in organic carbon), microbial dissimilated reduction by phosphorus, and Fe^{3+} hydroxides near the continental shelf. Although there is no consensus on the sources of iron in BIFs, the generally accepted view is that iron comes from two sources, namely, submarine hydrothermal activities and continental weathering, or a combination of both processes.

Submarine Hydrothermal Sources

Previous studies indicated that BIFs and hydrothermal fluids that originated from the mid-ocean ridge shared similar REE characteristics (such as positive Eu anomaly), and it was speculated that the iron mainly came from the submarine hydrothermal vents. Saito et al. (2013) supported the view by direct observations of iron-containing hydrothermal fluids from mid-ocean ridges. Nd isotopes can be used to trace the origin of iron in BIFs (Viehmann et al., 2014; Cox et al., 2016). Generally, hydrothermal fluids display high Sm/Nd ratios and positive Nd isotope values similar to mantle source materials, whereas continental materials usually show crustal characteristics with low Sm/Nd ratios and negative Nd isotope values. Nd isotopes of modern seawater are similar to those of river water and atmospheric dust, reflecting the addition of terrigenous detrital materials (Viehmann et al., 2014). Alexander et al. (2009) demonstrated that BIFs older than 2.7 Ga usually have relatively uniform εNd(t) (Nd model age) values ranging from +1 to +2, which is a typical Nd isotope characteristic of deep seawater dominated by submarine hydrothermal fluids (Viehmann et al., 2014).

Terrigenous Sources

The iron input from rivers contributes most of the iron sources to the modern ocean as a colloid or dissolved state and precipitates quickly on the continental shelf without effectively participating in the marine iron cycle (Poulton et al., 2002). In the early diagenetic process, iron is activated and re-migrated under the influence of the transformation of the redox environment in the pore water of sediments or the upper water, which is a very important part of the marine iron cycle. Previous studies on Nd isotopes of BIFs show that εNd(t) values of BIFs are mostly between the depleted mantle and the continental crust (Fig. 5), suggesting that seawater may be an important source of iron for BIFs. Based on Nd and Fe isotope data and REE characteristics of sedimentary sequences in Hamersley Basin, Western Australia, Li et al. (2015) summarize the two-source model of the origin of BIFs: (i) BIFs have high εNd and negative δ^{56}Fe values, indicating hydrothermal end-member components and (ii) the relatively low εNd and δ^{56}Fe values reflect the contribution of continental materials, transported to deep-basin sediments through iron migration by microorganisms under reducing conditions. Except for the abiogenic Fe from extensive shallow marine hydrothermal sources, biogenic Fe is also an important source, and the proportion of the two sources varies with the scale and time of the basin water cycle. Similar to the source of iron, it is recognized that silicon in BIFs is derived from both submarine hydrothermal fluid and continental

physical weathering. According to the different Nd isotopic compositions and Ge/Si ratios between seafloor hydrothermal fluid and terrigenous materials, it is proposed that the sources of silicon and iron are decoupled (Hamade et al., 2003; Frei et al., 2007), namely, iron comes mostly from submarine hydrothermal fluids, whereas silicon comes mostly from the continent's material weathering.

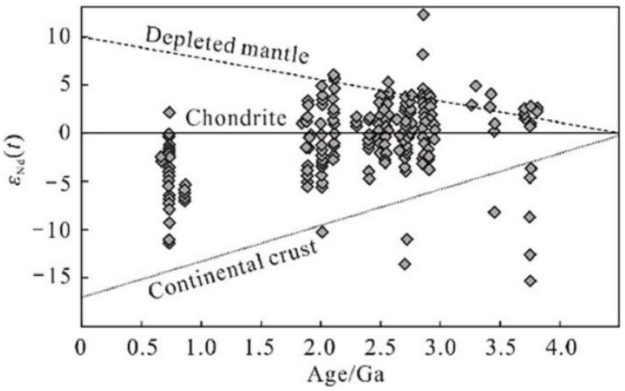

Fig. 5. Summary of εNd(t) isotope data of BIFs through Earth's history (Source: Yin et al., 2023).

Genesis

The classical and most widely accepted model for Fe formation deposition invokes ambient free oxygen (O_2)-induced ferrous Fe oxygenation. This model, championed by Cloud (1965), suggests that deposition of Fe formation occurred at the interface between oxygenated shallow waters and upwelling Fe-rich reduced waters. The oxidizing shallow waters have been linked to prolific communities of oxygenic photo-synthesizers (Cloud, 1965, 1968, 1973). It is supposed that three basic conditions are required for the vast deposition of iron in the ocean (Bekker et al., 2010; Planavsky et al., 2010): (1) atmospheres with lower oxygen fugacity (Holland, 1984); (2) sulfate and low sulfide concentrations (Habicht et al., 2002); and (3) high-temperature hydrothermal fluids (Klein, 2005). Cox et al. (2013) proposed that there were three conditions for the formation of Neoproterozoic BIFs: (1) Anoxic seawater keeps Fe^{2+} soluble, which is favourable for the accumulation and deposition of iron. The concentration of iron in modern seawater is very low, and its retention time is short about 1 to 100 years. Iron is highly soluble and has a long retention time in anoxic and sulfate-poor environments, such as the Archean Ocean. (2) The hydrogen sulfide to ferrous iron ratio is less than 2 ($H_2S/Fe^{2+} < 2$). If $H_2S/Fe^{2+} > 2$, Fe^{2+} is efficiently converted to pyrite, and the concentration of dissolved iron in seawater decreases. Therefore, the seawater constitutes an anoxic and iron-rich environment ($H_2S/Fe^{2+} < 2$) rather than an anoxic and sulfide environment (Cox et al., 2013). (3) The oxidation mechanism functions, i.e., the formation of $Fe(OH)_3$ by biological or abiotic oxidation processes from large amounts of dissolved Fe^{2+} in seawater occurs (Bekker et al., 2010). Based on a previous study and in combination with the latest research, we conclude that the formation of BIFs requires the following three conditions: (1) a substantial marine iron reservoir; (2) a reduction in the water environment, although the whole water does not need to be reduced; (3) that the Fe^{2+} precipitation mechanism functions, i.e., Fe^{2+} precipitation to form the original $Fe(OH)_3$.

Marine Anoxia vs. Oxidation

The BIFs record the chemical composition and redox state of the ancient oceans. The abundance of BIFs in the early Precambrian indicated the prevalence of anoxic, iron-rich oceans. Ce has two valence states (Ce^{3+} and Ce^{4+}) and is widely used as a redox indicator for sedimentary basin seawater due to its sensitivity to a redox environment (Cox et al., 2013; Planavsky et al., 2010). In most Precambrian BIFs, no obvious negative Ce anomaly was observed, indicating that the BIFs were mainly formed in the hypoxic environment (Cox et al., 2013). In oxidized seawater, the iron retention time is short and its concentration is low, whereas, in an anoxic environment, the iron retention time is long, and biological or abiotic oxidation would trigger iron precipitation, which displays significant iron isotope fractionation (Raye et al., 2015). Significant fractionation of iron isotopes can be observed in most Precambrian BIFs, indicating the partial oxidation of iron in a hypoxic or anoxic sedimentary environment (Hou et al., 2017). The modern ocean has a very low iron concentration of only 0.6 nmol/L (Conway et al., 2016; Thibon et al., 2019). The concentration of iron in the Proterozoic Ocean was 50 μmol/L (Raiswell et al., 2012), whereas the solubility of iron before GOE was higher and reached 100 μmol/L in the Archean Ocean (Sumner, 1997), which triggered the vast accumulation and precipitation of dissolved ferrous iron. Although BIFs were mainly formed in the early Precambrian, the oceanic redox

environment of the early Precambrian dynamically fluctuated (Huston et al., 2004). Holland (1984) suggested that the Neoproterozoic deep sea redeveloped from the high-oxygen fugacity to the medium-reducing environment, while Canfield (1998) asserted that the Neoproterozoic deep sea changed from the highly reducing condition to the medium-reducing condition and that the deep sea was an iron-rich environment. In conclusion, the deposition of BIFs does not require the entire seawater anoxia. The deposition of BIFs spans major processes in the early evolution of the Earth, from an early CO_2 and CH_4 dominated atmosphere to a CO_2 rich atmosphere (Bekker et al., 2007), suggesting that Precambrian BIFs can be formed through different oxidation pathways followed as,

Abiotic pathways

Based on the iron silicates present in BIFs today, some studies have argued that the origin of the primary minerals in BIFs was purely abiotic. Harder (1976, 1978) observed that nontronite or chamosite, two iron silicates observed in iron-rich formations, could be abiotically formed during anoxic, low-temperature synthesis of poorly crystalline Fe(III) oxyhydroxides from dissolved Fe(II) in the presence of silica. Harder (1976, 1978) and Konhauser et al. (2007) supported the formation of Fe-silicates in anoxic, non-sulfidic media with high dissolved Fe(II) and silica concentrations. Amongst the abiotic pathways, one of the proposed hypotheses suggests that Fe(II/III) silicates, particularly greenalite ($(FeII,FeIII)_2$-$3Si_2O_5OH_4$), was the main primary iron mineral and that it was deposited as nm-sized mud particles or loose flocs due to co-nucleation of Fe(II) and silica (Rasmussen et al., 2013, 2015b, 2019a). According to this hypothesis, current BIF mineralogy would, therefore, be explained by diagenetic, metamorphic, or weathering overprinting (Rasmussen et al., 2019b). One limitation of this pathway is the high pH value (7.5–8) necessary for the formation of Fe silicates, which is at odds with the assumed slightly acidic to circumneutral pH of the ocean at that time. Further, it has been shown that secondary oxidation of Fe-silicates, either through percolating oxidizing fluids or weathering, is not able to oxidize sufficient amounts of Fe(II) necessary to explain all the Fe(III) in BIFs on reasonable time scales. A second prevalent hypothesis concerning the abiotic formation of BIFs is the photochemical oxidation of dissolved Fe(II) (Fig. 6.1). Due to the lack of an ozone layer in the atmosphere, solar UV radiation was not attenuated. Therefore, dissolved Fe(II) in the photic zone might have adsorbed UV light, at wavelengths from 200 to 400 nm, resulting in the photochemical oxidation of ~ 0.07 atoms of dissolved Fe(II) per photon (Nie et al., 2017) and the formation of Fe(III). However, the photooxidation pathway has been challenged by experimental studies examining the effect of aqueous chemistry on UV photochemical oxidation. Konhauser et al. (2007) observed experimentally that at high dissolved silica and bicarbonate concentrations, the photooxidation of Fe(II) by UV light was substantially inhibited. This inhibition would suggest that photochemical oxidation, compared to other deposition pathways, only played a minor role in BIF deposition.

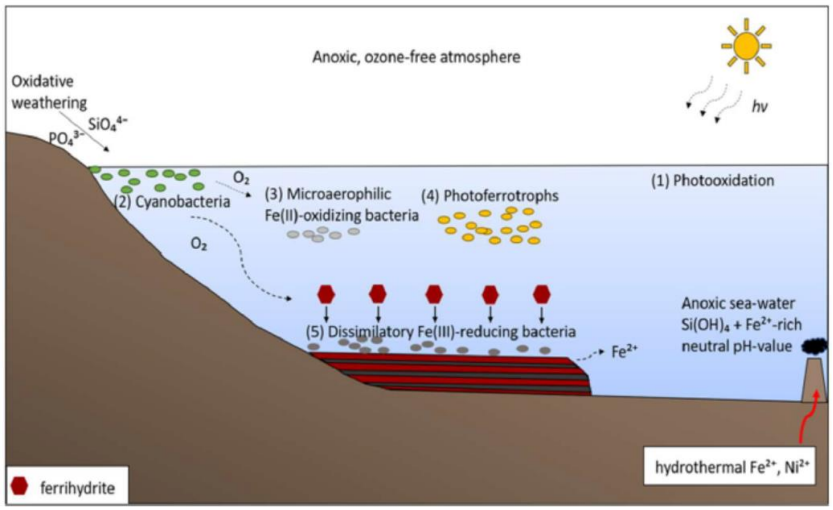

Fig. 6. Overview of biotic & abiotic BIFs deposition mechanisms. (1) Abiotic photooxidation of Fe(II) by UV radiation; (2) O_2 produced by cyanobacteria leading to abiotic oxidation of dissolved Fe(II); (3) Microaerophilic Fe(II)-oxidizing bacteria reducing O_2 produced by cyanobacteria for direct oxidation of Fe(II)(aq) to Fe(III) minerals; (4) Direct oxidation of dissolved Fe(II) by phototrophic Fe(II)- oxidizing (photoferrotrophic) bacteria and (5) Partial reduction of deposited Fe(III) minerals to mixed valence state Fe(II)Fe(III) minerals by dissimilatory iron(III)-reducing bacteria (DIRB) (Source: Dreher et al., 2021).

Biotic pathways

The majority of past work looking at biological pathways of BIF formation has focused on the role of cyanobacteria (Fig. 6.2). Fe(III) has been hypothesized to be formed via the chemical oxidation of dissolved Fe(II) by oxygen produced by cyanobacteria under circumneutral pH conditions (Cloud, 1973; Konhauser et al., 2007) and minerals such as ferrihydrite ($Fe(OH)_3$) are presumed to have been the dominant primary mineral. Once free oxygen became available in the ocean, other microorganisms, such as neutrophilic microaerophilic Fe(II)-oxidizers (Fig. 6.3), may have evolved and further contributed to Fe(III) mineral deposition by direct (enzymatically driven) Fe(II) oxidation. There are several lines of evidence suggesting that BIF formation may not be limited to cyanobacteria (Garrels et al., 1973). The assumption that cyanobacteria played a role in BIF deposition is partially founded on microfossils in the Precambrian sedimentary record. However, the dating of the first cyanobacterial occurrence in these formations is highly debated, as some of the oldest microfossils are not unambiguously primary or secondary in nature (Schirrmeister et al., 2016). Additionally, cyanobacteria might have suffered from ultraviolet irradiation and/or Fe(II) toxicity and potentially severe nutrient (e.g., phosphorous) limitations. These factors would have presented significant obstacles for early cyanobacteria and raised questions regarding the role cyanobacteria had in early BIF formation. Alternatively, Garrels et al. (1973) proposed that a different microbial process may have been responsible for the oxidation of the Fe(II), even under anoxic conditions: anoxygenic, photoautotrophic Fe(II) oxidation (photoferrotrophy) (Fig. 6.4). Photoferrotrophic bacteria use Fe(II) as an electron donor coupled to CO_2 fixation in the presence of light, resulting in the precipitation of Fe(III) and the formation of biomass. Their habitat reaches water depths of up to 100 m, facilitating BIF deposition even in the simultaneous presence of cyanobacteria in the overlaying water column (Kappler et al., 2005). Indeed, work by Konhauser et al. (2002) suggests that bacteria, and especially photoferrotrophic bacteria, could have deposited most, possibly even all, Fe contained in BIFs today. Although anoxygenic phototrophs may also be negatively affected by nutrient (e.g., phosphorus) limitations, this effect would be less severe than that on cyanobacteria. Another potential microbial metabolism contributing to direct Fe(III) precipitation, is nitrate-dependent Fe(II) oxidation. However, the presence of oxidized species, such as nitrate, in seawater is dependent on higher oxygen availability than assumed for Precambrian oceans (Oshiki et al., 2013). A major contribution to BIF deposition by these bacteria is, therefore, considered unlikely. Although indisputable conclusive evidence for the role of microorganisms in BIF deposition has not been found, there are several lines of direct and indirect evidence that support this hypothesis.

Iron ore deposits in India and their economic significance

Geological Set up

Banded Iron Formation (BIF) and iron ore deposits occupy three distinct provinces surrounding the North Odisha Iron Ore Craton (NOIOC) located in eastern India. These are BIF-I, BIF-II, and BIF-III chronologically from older to younger. The Bonai-Keonjhar belt (BIF-III) is located in the western flank, the Badampahar-Gorumahisani-Suleipat belt (BIF-I) in the eastern flank and Daitari-Tomka belt (BIF-II) in the southern side of the Craton. They are confined to the intracratonic rift basins of the early Proterozoic along the peripheral margin of NOIOC that form the Iron Ore Super Group (IOSG) of Odisha. The three-tier BIF-hosted iron ore-bearing formations are distinguished from each other by different metamorphic grades, distinct sedimentary and igneous assemblages, structural elements, and ore types, and are separated by unconformity. These tectonically evolved basins could accumulate volcanics of mafic to acid-intermediate composition, volcaniclastics, and chemical precipitates from terrestrial sources through continental denudation; from seawater through transgression and regression; from deep circulation of marine or meteoric water and from volcanic exhalation inside the basin. In the southern part of the NOIOC, the BIF-II is overlain by Dhanjori quartzite that extends northward along the western periphery up to BIF-III and underlies it. A separate quartzite formation (may be part of Mahagiri quartzite) underlying the BIF-II runs northward along the eastern flank of NOIOC up to BIF-I and overlies it. This quartzite may have a separate stratigraphic entity, which differs from the Dhanjori quartzite and is named Badam quartzite. The stratigraphic succession of IOSG constituting BIF-I, BIF-II, and BIF-III has been established (Table 1).

BIF-I: Badampahar-Gorumahisani Suleipat (BGS) Belt: BIF-I comprising of iron formation and iron ore is well developed at the BGS belt and part of it is discontinuously exposed along the southern hemisphere of the craton out skirting the BIF-II. The litho assemblages of this oldest Iron Ore Group under IOSG consist of banded cherty quartzite, banded magnetite quartzite, banded magnetite grunerite quartzite, tremolite-actinolite schist, and fuchsite quartzite. The Badam quartzite is well-exposed and overlies the BIF-I. Banded magnetite quartzite is

the dominant litho-unit in the BIF-I. The major mineral constituents are magnetite, martite, hematite, specularite, goethite, grunerite and quartz. The BIF-I has suffered amphibolite facies of metamorphism.

Table 1. Stratigraphic succession of Iron Ore Super Group of Odisha (Beura, 2014).

	Kolhan Group	Kolhan sediments (Sandstone, Limestone, Shale)	
	Unconformity		
IRON	Bonai-Keonjhar Group (BIF-III)	Upper Shale	Fe-shale banded shales
		BIF-III	Banded Hematite Chert/Jasper and banded hematite shale
ORE		Lower Shale	Banded shale Banded Manganese Formations (B Mn F) Variegated shales Tuffs & Tuffaceous shale
SUPER	Unconformity		
	Dhanjori Group		Dhanjori Volcanics Dhanjori Quartzite
GROUP	Unconformity		
(NOIOC)	Daitari-Tomka Group	Upper Metapelites	Phyllites Slate Fe-Phyllites
		BIF-II	Banded Chert Banded Magnetite/Hematite Chert/Jasper and Banded Magnetite/Hematite Quartzite
		Lower Metapelites	Banded Phyllites Quartz Schist Chlorite schist
	Unconformity		
	Badamphar- Gorumahisani- Suleipat Group	Upper Quartzite	Badam Quartzite Micaceous Quartzite
		BIF-I	Banded Magnetite/Martite Quartzite Banded Magnetite/Grunerite Quartzite
		Lower Quartzite	Banded black and green chert Tremolite-actinolite schist Fuchsite Quartzite
	Non- conformity		
PRE-IOSG PRE- CAMBRIAN	Singhbhum Granite≅Keonjhar granite ≅Bonai granite) (older to BIF-I) Tonalite gneiss (OMTG) OMG (Mica schist, fuchsite quartzite, Para-amphibolite, Hornblende-schist etc.)		

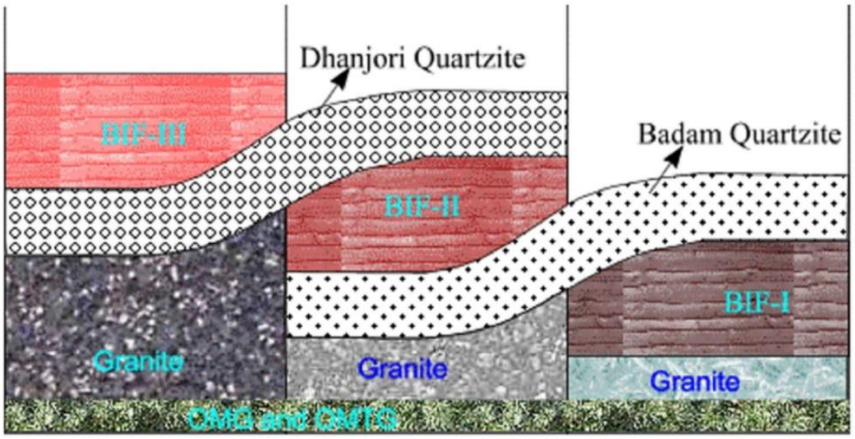

Fig. 7. Schematic diagram shows the stratigraphic setting of three BIFs of IOSG with respect to Badam and Dhanjori quartzite (Source: Beura et al., 2016).

BIF-II: Daitari-Tomka Belt: The BIF-II lying in the southern sector of the NOIOC is confined to the Daitari-Tomka belt. It is underlain and overlain by Badam quartzite and Dhanjori quartzite respectively (Fig. 7). The litho-assemblages are banded magnetite/hematite quartzite, banded magnetite/hematite jasper, quartz sericite schist, phyllites, slate and banded chert and the dominant minerals of the area are magnetite, martite, hematite and goethite. The rocks of BIF-II attain greenschist facies of metamorphism.
BIF-III: Bonai-Keonjhar Belt: BIF-III occupies a distinct 'U'-shaped pattern in the western flank of the NOIOC that rests over the Dhanjori Quartzite. The litho associations of this area are banded hematite jasper, banded hematite quartz/chert, banded shale, banded manganese formation, and ferruginous shale. The banded iron formation consists of predominantly iron oxide minerals such as hematite, martite, specularite, and magnetite, and silica such as chert, jasper, and quartz. The litho-assemblages of this youngest Iron ore belt are unmetamorphosed.

Different types of iron ores
Iron ore minerals associated with Precambrian banded iron formations are mainly found in three oxyhydroxy phases hematite, martite, and goethite. The different types of iron ores are described in the following sections.
Banded hematite jasper (BHJ): In banded hematite jasper, hematite is characterized by alternating bands/laminations with jasper. Bands are generally parallel and continuous but the 'pinching and swelling' feature is also recorded. Some of the samples are martitized revealing a relict magnetite phase in these rocks.

Massive ore: Hematite grains are fine-grained and tightly packed forming a compact mass in this type of ore. Martite is very common in this type of ore. Fine-to-medium-grained martite and microplaty crystals of hematite (specularite) are intricately associated with each other leaving very fine intergranular micropore spaces.

Hard laminated ore: Hard laminated ores are steel grey in colour and are relatively high grade. They consist of massive hematite with bands of specular hematite which exhibit a similar pattern as BHJ. The presence of microfractures in alternating bands confirms their origin from BHJ. During the formation of hard laminated ore, the secondary hematite emplacement occurs in the place of the Jasper band of BHJ. Further, the presence of very minor silica in the interstitial spaces strongly indicates their formation from BHJ.

Martite-goethite ore: In this type of ore, martite is the prominent iron-bearing minerals along with goethite which occur as voids and cavities. Precipitation of goethite in the voids has resulted due to the leaching out of pre-existing minerals.

Soft laminated ore: In this type of ore, individual lamellae measure from a few millimeters to centimeters in thickness and the ore is highly porous and fragile. The principal ore and gangue minerals are the same as those of hard-laminated ore. They are relatively rich in goethite, kaolinite, and gibbsite. The texture of soft laminated ore is almost similar to hard laminated ore but there are many voids between the lamellae, which are at times filled with secondary goethite and clay.

Goethitic-lateritic ore: Goethitic-lateritic ore is highly spongy and porous in nature. Goethite occurs as colloform bands and vein filling within the voids and cavities which is resulted due to the leaching out of pre-existing minerals.

Flaky-friable ores: Flaky-friable ore consists of hematite and martite as primary minerals and goethite, limonite, and gibbsite as secondary minerals. They are similar to soft laminated ore but have higher alumino-silicate minerals (kaolinite and gibbsite) compared to soft laminated ore.

Reserve potential and uses
The Indian BIFs are the primary hosts for the high-grade iron ores (> 60 wt. % of Fe) of the country. India is the sixth largest producer of iron ore in the world. At 55% cut-off grade for Fe (as per the release of the United Nations Framework Classification), the total resources of iron ore in India are expected to be around 28.52 billion tons of which about 17.88 billion tons of hematite and 10.64 billion tons are of magnetite ore as per records in Indian Mineral Year Book (2015). Furthermore, about 30% low grade including BHJ/BHQ iron ore (5.34BT) of total reserve is available for supply to Indian iron and steel industries. The BIF-hosted iron ore reserve occurs in almost all the major BIF-bearing successions of peninsular India. Almost 90% of hematite

resources occur in four states i.e., Orissa, Jharkhand, Chhattisgarh, and Karnataka. According to the National Steel Policy (2005) revised and reviewed subsequently in 2008 and 2012 to fix a target of 300 MTPA by 2025 of crude steel, it shall require 324 MTPA of processed ore and 505 MTPA of raw iron ore (Indian Bureau of Mines; Iron and Steel Vision 2020) and forecasts demand of iron will exceed supply by 22 million tons by the year 2016-2017. In order to overcome these issues, it is required to beneficiate the banded hematite jasper and banded hematite quartzite. Presently Several techniques such as washing, jigging, magnetic separation, advanced gravity separation, and flotation are being employed to enhance the quality of the Iron ore. Washing, jigging, and classification are being carried out for the beneficiation of Iron ores in India.

Conclusions

Our knowledge of BIF genesis is based on a combination of theoretical and geochemical models, analysis of the ancient rock record, and laboratory simulations of early Earth conditions. Although the lack of direct microfossil evidence makes it difficult to unambiguously identify a microbial role in BIF deposition, several independent lines of argument point towards the biogenicity of BIFs. Early- Proterozoic Ocean geochemistry, defined by its anoxic, iron and silica-rich environment, has been shown to be hospitable for several microbial metabolisms, including cyanobacteria, photoferrotrophs, and DIRB based on experimental studies. These microorganisms may have been the key players in Precambrian iron cycling in marine systems and ultimately led to the mineralogy we find in BIFs today. Accordingly, abiotic deposition mechanisms, such as direct Fe(II)-silica mineral precipitation (instead of Fe(III) minerals) and photooxidation of Fe(II), may have played a much smaller role than recently suggested. Iron formations around the NOIOC occupy different stratigraphic levels in the Precambrian. The grade of metamorphism decreases from bottom to top. The spatial disposition of these BIFs in space and time implies that the BIF-I, BIF-II, and BIF-III should be assigned an age status from old to young respectively. The different types of iron ores are intricately related to the BHJ. Removal of silica from BIF and successive precipitation of iron by hydrothermal fluids of possible meteoric origin resulted in the formation of martite-goethite ore. The hard laminated ore has been formed in the second phase of supergene processes, where the deep burial upgrades the hydrous iron oxides to hematite. The massive ore is syngenetic in origin with BHJ. Soft laminated ores and biscuity ores were formed where further precipitation of iron was partial or absent. In the present scenario, the Indian Steel industry is totally dependent upon high-grade iron ore. But in view of the ever-increasing demand for steel, the availability of iron ore resources (high grade) is depleting at a much faster rate. So, the necessity of Iron ore beneficiation is becoming a reality which is much more economical than getting rid of gangue at the higher end of the value chain like in an Electric furnace.

Acknowledgement: I am indebted to the major and precious contributions of legendary geoscientists around this globe to conceptualize and develop the origin of banded iron formation. The author is thankful to Dr. N. Chakraborty and Dr. A. Mondal for their critical comments during the revision. The author acknowledges Presidency University for its infrastructural support and would like to thank the Editor Dr. B. Mishra and the Associate Editor Dr. R. Nagendra.

References

Alexander, B.W., Bau, M. and Andersson, P. (2009). Neodymium isotopes in Archean seawater and implications for the marine Nd cycle in Earth's early oceans. Earth Planet. Sci. Lett., v.283, pp.144–155.

Bekker, A., Holland, H.D., Wang, P.L., Rumble, D., Stein, H.J., Hannah, J.L., Coetzee, L.L. and Beukes, N.J. (2004). Dating the rise of atmospheric oxygen. Nature, v.427(6970), pp.117–120.

Bekker, A. and Kaufman, A.J. (2007). Oxidative forcing of global climate change: A biogeochemical record across the oldest Paleoproterozoic ice age in North America. Earth Planet. Sci. Lett., v.258, pp.486–499.

Bekker, A., Slack, J.F., Planavsky, A., Krapež, B., Hofmann, A., Konhauser, K.O. and Rouxel, O.J. (2010). Iron formation: The sedimentary product of a complex interplay among mantle, tectonic, oceanic, and biospheric processes. Econ. Geol., v.105, pp.467–508.

Beura, D. (2014). Tectono-Structural Overviews of Iron Formation of North Odisha, India. Journal of Geosciences and Geomatics, v.2, pp.57-61.

Beura, D., Singh, P., Satpathy, B., Behera, S. and Nanda, S.K. (2016). Field Relationship among the Three Iron Ore Groups of Iron Ore Super Group Encircling the North Odisha Iron Ore Craton, India: A Comparison Study. Journal of Geosciences and Geomatics, v.4, pp.53-60.

Canfield, D.E. (1998). A new model for Proterozoic ocean chemistry. Nature, v.396, pp.450–453.

Cloud, P.E. (1965). Significance of the Gunflint (Precambrian) microflora. Science, v.148, pp.27–35.
Cloud, P.E. (1968). Atmospheric and hydrospheric evolution on the primitive Earth. Science, v.160, pp.729–736.
Cloud, P.E. (1973). Palaeoecological Significance of the Banded Iron-Formation. Econ. Geol., v.68, pp.1135–1143.
Conway, T.M., John, S.G. and Lacan, F. (2016). Intercomparison of dissolved iron isotope profiles from reoccupation of three GEOTRACES stations in the Atlantic Ocean. Mar. Chem., v.183, pp.50–61.
Cox, G.M., Halverson, G.P., Minarik, W.G., LeHeron, D.P., Macdonald, F.A., Bellefroid, E.J. and Strauss, J.V. (2013). Neoproterozoic iron formation: An evaluation of its temporal, environmental and tectonic significance. Chem. Geol., v.362, pp.232–249.
Cox, G.M., Halverson, G.P., Poirier, A., Heron, D.L., Strauss, J.V. and Stevenson, R. (2016). A model for Cryogenian iron formation. Earth Planet. Sci. Lett., v.433, pp.280–292.
Dreher, C.L., Schad, M., Robbins, L.J., Konhauser, K.O., Kappler, A. and Joshi, P. (2021). Microbial processes during deposition and diagenesis of Banded Iron Formations. PalZ, v.95, pp.593–610.
Evans, A.M. (1993). Ore Geology and Industrial Minerals_An Introduction, 3rd ed. Blackwell Science Ltd.
Frei, R. and Polat, A. (2007). Source heterogeneity for the major components of ~3.7 Ga Banded Iron Formations (Isua Greenstone Belt, Western Greenland): Tracing the nature of interacting water masses in BIF formation. Earth Planet. Sci. Lett., v.253, pp.266–281.
Garrels, R.M. Perry Jr., E.A. and MacKenzie, F.T. (1973). Genesis of Precambrian Iron-Formations and the Development of Atmospheric Oxygen. Econ. Geol., v.68(7), pp.1173–79.
Gole, M.J. and Klein, C. (1981). Banded Iron-Formations through Much of Precambrian Time. The Journal of Geology, v.89, pp.169-183.
Gross, G.A. (1965). Geology of iron deposits in Canada, Volume 1. General geology and evaluation of iron deposits, Geological Survey of Canada Economic Report, 22.
Habicht, K.S., Gade, M., Thamdrup, B., Berg, P. and Canfield, D.E. (2002). Calibration of sulfate levels in the Archean ocean. Science, v.298, pp.2372–2374.
Hamade, T., Konhauser, K.O., Raiswell, R., Goldsmith, S. and Morris, R.C. (2003). Using Ge/Si ratios to decouple iron and silica fluxes in Precambrian banded iron formations. Geology, v.31, pp.35–38.
Harder, H. (1976). Nontronite synthesis at low temperatures. Chemical Geol., v.18(3), pp.169–180.
Harder, H. (1978). Synthesis of Iron Layer Silicate Minerals under Natural Conditions. Clays and Clay Minerals, v.26(1), pp.65–72.
Heinrich, D., Holland, M. and Schidlowski, M. (1982). Mineral deposits and the evolution of the biosphere. Berlin, Heidelberg.
Hoffman, P.F. and Schrag, D.P. (2000). Snowball Earth. Sci Am., v.282, pp.68–75.
Holland, H. (1984). The Chemical Evolution of the Atmosphere and Oceans; Princeton University Press: New York, NY, USA, p.582.
Hou, K., Ma, X., Li, Y., Liu, F. and Han, D. (2017). Chronology, geochemical, Si and Fe isotopic constraints on the origin of Huoqiu banded iron formation (BIF), southeastern margin of the North China Craton. Precambrian Res., v.298, pp.351–364.
Huston, D.L. and Logan, G.A. (2004). Barite, BIFs and bugs: Evidence for the evolution of the Earth's early hydrosphere. Earth Planet. Sci. Lett., v.220, pp.41–55.
James, H.L. (1954). Sedimentary facies of iron-formation. Econ. Geol., v.49, pp.235–249.
James, H.L. and Sims, P.K. (1973). Precambrian iron formations of the world. Econ. Geol., v.68, pp.913-4.
James, H.L. and Trendall, A.F. (1982). Banded iron formation: distribution in time and palaeoenvironmental significance. In: Holland, H.D. & Schidlowski, M. (eds), Mineral Deposits and the Evolution of the Biosphere, pp.119-218. Springer-Verlag, Heidelberg.
Kappler, A., Pasquero, C., Konhauser, K.O. and Newman, D.K. (2005). Deposition of banded iron formations by anoxygenic phototrophic Fe(II)-oxidizing bacteria. Geology, v.33(11), pp.865–868.
Klein, C. (2005). Some Precambrian Banded Iron Formations (BIFs) from around the world: their age, geologic setting, mineralogy, metamorphism, geochemistry, and origin. Am. Mineral., v.90, pp.1473–1499.
Konhauser, K.O., Hamade, T., Raiswell, R., Morris, R.C., Ferris, G.F., Southam, G. and Canfield, D.E. (2002). Could bacteria have formed the Precambrian banded iron formations? Geology, v.30(12), p.1079.
Konhauser, K.O., Lalonde, S.V., Amskold, L. and Holland, H.D. (2007). Was there really an Archaean phosphate crisis? Science, v.315(5816), p.1234.

Li, W., Beard, L. and Johnson, C.M. (2015). Biologically recycled continental iron is a major component in banded iron formations. Proc. Natl. Acad. Sci. USA, v.112, pp.8193–8198.

Mojzsis, S.J., Arrhenius, G., McKeegan, K.D., Harrison, T.M., Nutman, A.P. and Friend, C.R.L. (1996). Evidence for life on Earth before 3,800 million years ago. Nature, v.384, pp.55–59.

Mukhopadhyay, J. (2020). Archean banded iron formations of India. Earth-Science Reviews, v.201, p.102927.

Neukirchen, F. and Gunnar, R. (2020). The World of Mineral Deposits_A Beginner's Guide to Economic Geology- Springer.

Nie, N.X., Dauphas, N. and Greenwood, R.C. (2017). Iron and oxygen isotope fractionation during iron UV photo-oxidation: Implications for early Earth and Mars. Earth Planet. Sci. Lett., v.458, pp.179–191.

Oshiki, M., Ishii, S., Yoshida, K., Fujii, N., Ishiguro, M., Satoh, H. and Okabe, S. (2013). Nitrate dependent ferrous iron oxidation by anaerobic ammonium oxidation (anammox) bacteria. Applied and Environmental Microbiology, v.79(13), pp.4087–4093.

Planavsky, N., Rouxel, O., Bekker, A., Shapiro, R., Fralick, P. and Knudsen, A. (2009). Iron-oxidizing microbial ecosystems thrived in late Paleoproterozoic redox-stratified oceans. Earth Planet. Sci. Lett., v.286, pp.230–242.

Planavsky, N., Bekker, A., Rouxel, O.J., Kamber, B., Hofmann, A., Knudsen, A. and Lyons, T.W. (2010). Rare Earth Element and yttrium compositions of Archean and Paleoproterozoic Fe formations revisited: New perspectives on the significance and mechanisms of deposition. Geochim. Cosmochim. Acta, v.74, pp.6387–6405.

Pohl, W.L. (2011). Economic Geology Principles and Practice_Metals, Minerals, Coal and Hydrocarbons – Introduction to Formation and Sustainable Exploitation of Mineral Deposits- Wiley-Blackwell.

Poulton, S.W. and Raiswell, R. (2002). The low-temperature geochemical cycle of iron: From continental fluxes to marine sediment deposition. Am. J. Sci., v.302, pp.774–805.

Raiswell, R. and Canfield, D.E. (2012). The iron biogeochemical cycle past and present. Geochem. Perspect., v.1, pp.1–2.

Rasmussen, B., Meier, D.B., Krapež, B. and Muhling, J.R. (2013). Iron silicate microgranules as precursor sediments to 2.5 billion years old banded iron formations. Geology, v.41(4), pp.435–438.

Rasmussen, B., Krapež, B., Muhling, J.R. and Suvorova, A. (2015b). Precipitation of iron silicate nanoparticles in early Precambrian oceans marks Earth's first iron age. Geology, v.43(4), pp.303–306.

Rasmussen, B., Muhling, J.R. and Fischer, W.W. (2019a). Evidence from laminated chert in banded iron formations for deposition by gravitational settling of iron-silicate muds. Geology, v.47(2), pp.167–170.

Rasmussen, B., Muhling, J.R., Tosca, N.J. and Tsikos, H. (2019b). Evidence for anoxic shallow oceans at 2.45 Ga: Implications for the rise of oxygenic photosynthesis. Geology, v.47(7), pp.622–626.

Raye, U., Pufahl, P.K., Kyser, T.K., Ricard, E. and Hiatt, E.E. (2015). The role of sedimentology, oceanography, and alteration on the δ56 Fe value of the Sokoman Iron Formation, Labrador Trough, Canada. Geochim. Cosmochim. Acta, v.164, pp.205–220.

Saito, M.A., Noble, A.E., Tagliabue, A., Goepfert, T.J., Lamborg, C.H. and Jenkins, W.J. (2013). Slowpreading submarine ridges in the South Atlantic as a significant oceanic iron source. Nat. Geosci., v.6, pp.775–779.

Schirrmeister, B.E., Sanchez-Baracaldo, P. and Wacey. D. (2016). Cyanobacterial evolution during the Precambrian. International Journal of Astrobiology, v.5(3), pp.187–204.

Sumner, D.Y. (1997). Carbonate precipitation and oxygen stratification in late Archean seawater as deduced from facies and stratigraphy of the Gamohaan and Frisco formations, Transvaal Supergroup, South Africa. Am. J. Sci., v.297, pp.455–487.

Thibon, T., Blichert-Toft, J., Tsikos, H., Foden, J., Albalat, E. and Albarede, F. (2019). Dynamics of oceanic iron prior to the Great Oxygenation Event. Earth Planet. Sci. Lett., v.506, pp.360–370.

Trendall, A. F. (1965). Progress report on the Brockman Iron Formation in the Wittenoom-Yampire area: West. Aust. Geol. Surv. Ann. Rept., 1964, p.55-65.

Trendall, A.F. and Blockley, J.G. (1970). The iron formations of the Precambrian Hamersley Group, western Australia: Geological Survey of Western Australia Bulletin, 119, 366 p.

Viehmann, S., Hoffmann, J.E., Münker, C. and Bau, M. (2014). Decoupled Hf-Nd isotopes in Neoarchean seawater reveal weathering of emerged continents. Geology, v.42, pp.115–118.

Yin, J., Li, H. and Xiao, K. (2023). Origin of Banded Iron Formations: Links with Paleoclimate, Paleoenvironment, and Major Geological Processes. Minerals, v.13, p.547.